SIXTH EUROPEAN ROTORCRAFT AND POWERED LIFT AIRCRAFT FORUM

PAPER NO. 58

PARAMETER IDENTIFICATION OF A HINGELESS ROTOR HELICOPTER IN FLIGHT CONDITIONS WITH INCREASED INSTABILITY

M.Kloster

Messerschmitt-Bölkow-Blohm GmbH
München, Germany

J.Kaletka

Deutsche Forschungs- und Versuchsanstalt
für Luft- und Raumfahrt
Braunschweig, Germany

H. Schäufele

Messerschmitt-Bölkow-Blohm GmbH
München, Germany

September 16 - 19, 1980
Bristol, England

THE UNIVERSITY, BRISTOL, BS8 1HR, ENGLAND

PARAMETER IDENTIFICATION OF A HINGELESS ROTOR HELICOPTER IN FLIGHT CONDITIONS WITH INCREASED INSTABILITY

M.Kloster

Messerschmitt-Bölkow-Blohm GmbH
München, Germany

J.Kaletka

Deutsche Forschungs- und Versuchsanstalt
für Luft- und Raumfahrt
Braunschweig, Germany

H. Schäufele

Messerschmitt-Bölkow-Blohm GmbH
München, Germany

Abstract

The joint MBB and DFVLR research programme on parameter identification was extended to a second phase. In the first phase the helicopter was flown at about 70 kts and identified. In the second phase, flight conditions were selected in which the helicopter showed an increasing instability: the hover and flight at maximum speed. Both flight conditions were performed with maximum weight and a mid c.g. position.

Because of the instability, an attitude feedback control system was necessary. A strap-down system was selected as a compact measuring system. The closed loop stabilization was carried out by on-board-computer.

The input signals were optimized for the unstabilized helicopter. Calculations in the time and frequency domains, showed that special input signals for the closed loop system were needed. A special distribution of the power spectrum led to a quasi optimized input signal. The optimized input signals were filtered by linear filters of second order to suppress the dynamics of the rotor, which can be considered as perturbations or system noise.

The identified derivatives from flight test (6 DOF rigid body model) are compared with the identification results of non-linear simulation and the quasi static theory. Generally, the agreement is good.

1. Introduction

Parameter identification from flight test data of fixed-wing-aircraft is a common procedure nowadays and a useful tool in the development phase as well as in the certification of the airplane. The identification of rotorcraft parameters has been in the research stage up to now. This is

primarily due to adverse helicopter characteristics, such as nonlinearity, coupled behaviour, many degrees of freedom (for example: a 4-bladed rotor with flapping and lagging modes and a rigid body needs 326 coefficients to identify, see Reference 9), high vibration levels, inherent instabilities and measurement problems, such as airspeed measurement in transition flight.

As can be seen from Reference 1 to 9, many authors have performed basic work to establish a suitable identification procedure for rotorcraft. Tomaine et al. reported on the identification from flight test of a helicopter with articulated rotors (Reference 10). The identification from simulation and dynamic wind tunnel tests of a hingeless model rotor is presented in Reference 11.

Parameter identification results from flight tests of the MBB -BO 105 helicopter with a hingeless rotor are reported in Reference 12. This was the first one of two phases of the joint MBB and DFVLR research programme.

In the first phase the helicopter was flown with a small instability in the phugoid with a gross weight of 2100 kg and a forward c.g. position. The flight velocity was about 70 ktas. In the second phase, flight conditions were selected in which the phugoid of the helicopter showed an increasing instability: hover and level flight with maximum speed (about 130 ktas) at 5000 ft. Both flight conditions were performed at maximum gross weight (2300 kg) and a mid c.g. position.

Herein the necessary feedback control , the optimization of the input signal, and the chosen measuring equipment will be described and discussed, as well as a comparison of the identification results of simulated and flight test data with the theory.

2. Procedure and Methods of System Identification

The overall identification procedure, shown in Figure 1, includes four main phases: preparation, flight test, evaluation, and conclusions. In the preparation phase one must investigate simulations for yielding the best model for identification and input signals. Preparation of the flight test will be done: - For example the flight programme and the provision of necessary instrumentation. After flight tests, data recording and processing, the identification process can be started.

The identification methods usually applied are the equation error methods (Least Squares and Instrumental Variable), as well as the Maximum Likelihood technique. Equation error methods are computationally highly efficient and, therefore, very attractive for the identification of systems with many unknown parameters, like helicopters. Their application, however, requires accurately measured variables (especially acceleration) and no or only small disturbances, like wind or gusts.

Flight test data evaluated in this research programme had only relatively poor linear acceleration measurements. Therefore, only the more powerful Maximum Likelihood technique was used although it is computationally less efficient. This iterative method yields unbiased estimates of the unknown parameters. As it requires start up values, usually a priori values are used otherwise, it is necessary to obtain these values from some other identification methods, the Least Square identification for example. To

avoid this disadvantage, the Maximum Likelihood method was modified to start the identification without any a priori values at all. In addition, the possibility was provided of including well known a priori values of derivatives in the estimation criterion to improve both, accuracy and convergence of the identification.

For comparison only the Instrumental Variable method was used in the first phase of the programme.

After the evaluation phase (see Fig. 1) a conclusion stage is conducted, including comparisons of derivatives with theory, stability and control investigations, handling qualities, certification work, data storage, etc.

3. Helicopter Dynamics

3.1 Hover

Figure 2 shows the eigenvalues of the MBB-BO 105 helicopter in hover, obtained by a rotor model with the following degrees of freedom: flapping, lagging, blade torsion and a torsion mode due to the control flexibility. Because of transformation from the rotating system to the body axes two more eigenvalues per blade mode must be added. It should be mentioned, that the tail rotor and the fuselage are assumed not to behave dynamically.

In this programme the 6 DOF rigid body modes only should be identified, which yields finally, the phugoid, the Dutch roll, two short periods and a well damped roll mode. When calculating eigenvalues with rotor dynamics, this roll mode leads to a roll-flap-coupling. For the identification procedure all motions of the rotor dynamics together with the dynamics of the fuselage appears as system noise.

Figure 3 shows the eigenvalues of the 6 DOF rigid body system (Dutch roll, phugoid) as a function of small translational velocities, which can be achieved from the hover state by control input perturbations.

The mapping of this velocity-region (u = ±5 m/s, v = ±5 m/s) into the Gauss-plane shows unsymmetric behaviour of the Dutch roll and phugoid, and a change of frequency and damping. The identification calculation, however, can only produce mean values of the derivatives.

3.2 Forward Level Flight

Time histories of rigid body and rotor dynamics of the helicopter in forward flight at maximum speed (about 250 km/h) are given in Figure 4. A short impulse (.1 sec) was applied to all four controls. Rotor dynamics are approximated by

$$\psi = a_0 + a_1 \cdot \cos(\Omega t) + b_1 \cdot \sin(\Omega t),$$

where ψ stands for flapping angle β, or lagging angle ζ, or blade torsion angle Θ_B, or the torsion angle Θ_E due to the control flexibility. The "constants" in this equation are further time dependent.

Nearly all time histories show the strong effect of the rotor dynamics.

It is well known that an optimal design of control input signals yields a drastic reduction of this effect, which means lower system noise in the identification process. The lowest frequency to be avoided is the difference of flapping and rotor revolution ($\omega_\beta - \Omega$). The dependancy of the eigenvalues of this motion on flight velocity is shown in Figure 5. Later on, the optimization of input signals will be discussed, which leads to power spectra with a high level up to the frequency of 5 rad/sec and a low level for frequencies above 5 rad/sec.

The phugoid becomes increasingly unstable with increasing flight velocity. At maximum level speed there is a rapid aperiodic unstable motion. The time to double amplitude is close to 1 second. For the purpose of achieving a test time of about 15 seconds for data recording of one manoeuver, a feedback control had to be installed.

4. Feedback Control and Measuring Equipment

The necessary feedback control had to be as simple as possible. Only a stabilization of the phugoid had to be arranged. Figure 6 demonstrates the effect of pitch-attitude feedback on the phugoid root locus. An amplification factor of K_Θ = 0.1 to 0.15 deg/deg will stabilize the motion well enough for data recording of 15 seconds test duration.

The situation for stabilizing the motion at hover is given in Figure 7. Full stabilization is only possible with pitch- and roll-attitude feedback. The combination of the amplification factors K_Θ = 0.2 and K_φ = 0.05 deg/deg yields good stabilization.

For flight tests of advanced flight control and guidance systems MBB developed an in-flight-simulator which is fitted with a nonredundant fly-by-wire control system and a conventional mechanical control as the back up system (Reference 13). A flight test programme with a digital helicopter feedback control system and a strap-down system was performed previously (Reference 14). Because of availability and good test results, this system was again chosen for the measuring and feedback equipment. The architecture of the complete system is presented in Figure 8.

A preliminary study demonstrated that a sampling frequency of 40 Hz would be necessary for the linear accelerations and angular velocities, which was implemented.

5. Input Signal Optimization

Optimization of input signals is a common preliminary process in identification of system parameters, see References 8, 9, 12, 16 to 19. The idea is, to obtain a large power spectrum in the region of the system frequencies and to minimize the "system noise" coming from the dynamics of the rotor and of the fuselage-structure. Highest natural frequency of the 6 - degree-of-freedom system is near 1 rad/sec in hover, see Fig.2, and about 4 rad/sec in forward flight at maximum speed (Fig. 5). The lowest eigenvalue of the rotor dynamics is 3 rad/sec ($\omega_\beta - \Omega$) in the case of hover and 6 ÷ 7 rad/sec in the fast flight. For higher frequencies, the power spectra should show minimum content. The ideal spectral density is that of bandwidth limited white noise, which can be provided by a so called "impulse-sine" input signal with variable frequency and amplitude.

The more practical way is to find a series of step functions which leads to limited spectral density.

Figure 9 shows the power spectrum of the 3 - 2 - 1 - 1 signal, used in the first phase of MBB-BO 105 identification. Further optimization led to a seven-seconds-signal with a new step at every second. The power spectrum at frequencies lower than 5 rad/sec is better and for higher values it vanishes as well as the one of the 3 - 2 - 1 - 1 signal.

It should be mentioned, that this input signal optimization is valid only for an open loop system. Eigenvalues of closed loop systems change as well as derivatives. In this case, energy coming from pitching, and in hover also from rolling, is added into the controls. Therefore, the power spectrum will show a peak at the eigenfrequency of the new phugoid or Dutch roll. For that reason an input signal was designed, showing minimum power spectral density at this frequency. This is possible with a very simple 3 - sec - signal, see Figure 10. General organization of the controlled system is given in Figure 11. The peaks in the power spectra are shown in Figure 12 to 15. From the point of view of optimization input signals with respect to power spectral density, the 3 - sec. - signal (Figure 10) is superior to the optimized 7 - sec.-Signal (Figure 9) in forward flight. To suppress the excitation of the rotor dynamics in the hover flight test, it was necessary, to choose longer time steps. This results in a smaller power spectrum distribution.

All input signals were filtered by

$$F = \frac{1}{(1+T \cdot s)^2}$$

with $T = 0.1 - 0.3$ sec.

6. Computer Simulations

Computer simulations with a nonlinear model of the helicopter motion, including flapping of the rotor blade were implemented for the following reasons

- testing the feedback control
- evaluation of amplitudes of the control inputs
- provision of data for early identification to find out problems and an optimal linear model.

Input signals, flight conditions (hover, 200/230 km/h) and the sampling of the rotor-computation were varied. Figure 16 shows one of these simulations with the following inputs

- 2-sec-doublet in longitudinal control
- 2-sec-doublet in tail rotor collective pitch
- 7-sec-optimized signal in lateral control
- 4-sec-doublet in main rotor collective pitch.

All movements are in the flight regime which allows linearization. Tail rotor control input has a significant influence on yawing. The main rotor collective pitch input effects pitching and rolling as well as vertical

acceleration. The effect of rotor dynamics (flapping) can be seen from the time histories of foreward (DVXG/DT) and sideward (DVYG/DT) acceleration.

7. Flight Tests

The overall flight test programme lasted about ten hours for check - and measuring flight with 145 manoeuvers of about 15 - 20 seconds duration. The test vehicle MBB-BO 105 (modified version) with a hingeless four bladed rotor has a fly-by-wire control and a mechanical back up control system. Figure 17 shows this rotorcraft with the installed strap-down system at the loading platform.

During flight the test pilot could choose the amplification factors of the feedback system in the digital flight control unit (Figure 18), as well as the input signals (5 different were available) and the time constants of the filter, Figure 19. All tests were controlled in a telemetry station.

They were conducted with the following flight conditions:

Gross weight (take off)	2350 kg
c.g.position	mid
density altitude	5000 ft
trim speeds	200 ÷ 240 km/h
hover	200 ft above ground

8. Data Processing

Flight test data obtained from the strap-down measuring system were recorded on magnetic tape on board of the helicopter. The data contained many spikes, probably due to helicopter vibration effects on the tape recorder. Therefore, when the data had been transferred to a digital computer, main emphasis was initially on automatically detecting and eliminating these drop outs.

Figure 20 (left) shows pitch rate measurements with data spikes. The same data are shown in Figure 20 (right) with drop outs eliminated and substituted by interpolated data.

Another flight test data problem area was drift in the speed components (Figure 21) and, to a lesser extent, in the attitude angles. This drift was not corrected for as the identification procedure itself estimates time history drifts. It complicated the accurate definition of steady state flight conditions prior to each test run. This is particularly important when multiple run evaluation is applied or when results, obtained from different runs, are compared.

The third problem is poor quality of the horizontal linear acceleration measurement, see Figure 22 (left) for example. The vertical acceleration is good enough, as seen in Figure 22 (right).

9. Identification Results

This section presents the results obtained from Maximum Likelihood identification of simulated and flight test data. Initially, the 6-DOF-model was identified with all derivatives, but some were dropped. Finally, the following model led to acceptable results

	u	v	w	p	q	r
X	x	0	x	0	$-w_0 q$	0
Y	0	x	x	$w_0 p$	0	$-u_0 r$
Z	x	0	x	0	$u_0 q$	0
L	x	x	x	x	x	0
M	x	x	x	x	x	0
N	0	x	0	0	0	x

X identified derivative

0 no derivative

Time histories of multiple run results of hover are shown in Figure 23. The results of forward flight are given in Figure 24. Identification curves correlate frequently with flight test data.

The most important derivatives, identified from simulated and flight test data, are compared with theory of 2300 kg/mid c.g.position and of 2100 kg/forward c.g.position in Figure 25.

Force Derivatives. The longitudinal force derivatives X_u due to speed change show good agreement with theory. The result from flight test, however, shows a large standard deviation. Also the identified derivatives Y_v agree reasonably well with theoretical calculations, but the vertical damping Z_w seems to be smaller than calculated (forward flight). The identification from simulated data deviates from theory and flight test data identification (hover).

Rolling Moment Derivatives. The derivatives of dihedral effect L_v are close to the calculated as well as the results of simulation. Roll damping L_p from flight test identification is smaller than predicted calculation (forward flight). Another identification process with the complete 6-DOF-model and fixed derivatives X_v, Y_q, Z_p, L_v, M_p from theory showed better agreement of the identified L_p-derivatives with the theoretical values. All results from hover are close together. The coupling derivatives L_q shows large scatter, but the tendency is in agreement with theory, except at 200 km/h and hover.

Pitching Moment Derivatives. All identified derivatives of speed stability M_u harmonize with the theoretical curve except the identified simulation of hover. It should be mentioned that only the best results of identification of simulated data were taken. The derivatives of angle of attack stability (M_w) are smaller than those from theory. Forward c.g.position (2300 kg) results in smaller M_w-values, which can be seen from the M_w-plot. Hover simulation drops out again. Also the pitch damping M_q shows smaller values and the same behaviour with increasing speed as the coupling derivative M_p.

Yawing Moment Derivatives. Directional stability and yaw damping were the only derivatives considered during the identification procedure. The directional stability derivatives N_v at hover agree with calculated values, but in forward flight, only smaller values were obtained. Other MBB flight tests showed, that theory seems to produce better directional stability. Yaw damping N_r is smaller when identified from flight test than calculated results at hover point, but near predicted curves in forward flight.

Control Derivatives. The following table shows some of the obtained control derivatives. Most of the identified derivatives show fair agreement with those of theoretical calculations.

	THEORY			IDENTIFICATION FROM NON LIN. SIMULATION		FLIGHT TEST			DIM.
	HOVER	200	240	HOVER	200	HOVER	200	240	KM/H
$Z_{D\theta}$	-1.3	-2.2	-2.1	-1.3	-1.6	-1.1	-0.9	-	M/S²GRD
$L_{D\alpha'}$	+2.8	+2.7	+2.7	+2.0	+2.3	+1.8	+0.8	+1.9	1/S²GRD
$M_{D\theta}$	0	+0.6	+0.7	+0.04	+0.4	+0.1	+0.5	-	1/S²GRD
$M_{D\beta}$	+0.9	+1.0	+1.1	+0.4	+0.7	+0.4	+0.3	+0.3	1/S²GRD
$N_{D\delta}$	-0.2	-0.4	-0.3	-0.2	-0.4	-0.2	-	-	1/S²GRD

Most identification results were obtained from flight test data without making use of any a priori values of the derivatives to be identified. For the hover condition, however, an a priori weighting technique was applied for those derivatives that were quite accurately known from theoretical quasi static calculations. Weighting factors were selected in such a way to allow significant deviations of the identified derivatives from the a priori values.

10. Conclusion

The joint MBB and DFVLR research programme on parameter identification of the hingeless helicopter MBB-BO 105 was extended to flight conditions with increased instability: hover and level flight with maximum speed.

The measuring equipment used was a strap-down system. Data recording and processing technique proved to be adequate, but a higher sampling would yield better results.

Identification of a controlled helicopter is possible and showed no identification problems. Optimization of input signals was extended, especially for the controlled system. The good agreement of theoretical and identified derivatives indicates a high standard of the theoretical tools.

11. References

1. Molusis, J.A. — Rotorcraft Derivative Identification from Analytical Models and Flight Test Data, AGARD Flight Mechanics Panel Specialists Meeting, Hampton U.S.A. 5-8.11.1974

2. Molusis, J.A. — Helicopter Stability Derivative Extraction and Data Processing Using Kalman Filtering Technique, 28 th Annual National Forum of the American Helicopter Society, 1972

3. Molusis, J.A. — Helicopter Stability Derivative Extraction from Flight Data Using the Bayesian Approach to Estimation, Journal of the American Helicopter Society, July 73

4. Molusis, J.A. — Analytical Study to Define a Helicopter Stability Derivative Extraction Method - Final Report, NASA-CR-1323 72, United Aircraft Corp., 1973

5. Hall, W.E.Jr. Gupta, N.K. Hansen, R.S. — Rotorcraft System Identification Techniques for Handling Qualities and Stability and Control Evaluation, 34 th Annual National Forum of the American Helicopter Society, 1978

6. Gould, D.G. Hindson, W.S. — Escimates of the Stability Derivatives of a Helicopter from Flight Measurements 9 th ICAS Congress, Haifa, Israel, August 1974

7. Johnson, W. Gupta, N.K. — Transfer Function and Parameter Identification Methods for Dynamics Stability Measurement, 33rd Annual National Forum of the American Helicopter Society, Washington, 1977

8. Kaletka, J. Rix, O. — Aspects of System Identification of Helicopters, 3rd European Rotorcraft and Powered Lift Aircraft Forum, Aix-en-Provence, France, 1977

9. Kaletka, J. — Rotorcraft Identification Experience, AGARD Lecture Series No. 104, Delft, 1979

10. Tomaine, R.L. Bryant, W.H. Hodge, W.F. — VALT Parameter Identification Flight Test, 4th European Rotorcraft and Powered Lift Aircraft Forum, Stresa, Italy, 1978

11. Kanning, G. Biggers, J.C. — Application of a Parameter Identification Technique to a Hingeless Helicopter Rotor, NASA D-7834, 1974

12. Rix, O. Huber, H. Kaletka, J. — Parameter Identification of a Hingeless Rotor Helicopter, 33rd Annual National Forum of the American Helicopter Society, Washington, D.C., 1977

13. Attlfellner, S.
Rade, M.
BO 105 In-Flight Simulator for Flight Control and Guidance Systems,
1. European Rotorcraft and Powered Lift Aircraft Forum, Southampton, 1975

14. Kubbat, W.J.
Evaluation of a Digital Helicopter Control System,
3rd European Rotorcraft and Powered Lift Aircraft Forum, Aix-en-Provence, France, 1977

15. Tomaine, R.L.
The Effect of Pilot Control Input Shape on the Identification of Six Degree-of-Freedom Stability and Control Derivatives of a Transport Helicopter,
Master's Thesis, George Washington University, Washington, D.C., 1976

16. Plaetschke, E.
Schulz, G.
Practical Input Signal Design,
AGARD Lecture Series No. 104, 1979

17. Mekra, R.K.
Gupta, N.K.
Status of Input Design for Aircraft Parameter Identification,
AGARD-CP-172, 1975

18. Chen, R.T.N.
Input Design for Aircraft Parameter Identification: Using Time-Optimal Control Formulation,
AGARD-CP-172, 1975

19. Marchand, M.
Koehler, R.
Determination of Aircraft Derivatives by Automatic Parameter Adjustment and Frequency Response Methods,
AGARD-CP-172, 1975

20. Reichert, G.
Basic Dynamics of Rotors: Control and Stability of Rotary Wing Aircraft: Aerodynamics and Dynamics of Advanced Rotary Wing Configurations,
AGARD-LS-63, 1973

21. Huber, H.
Some Objectives in Applying Hingeless Rotors to Helicopters and V/STOL Aircraft,
AGARD-CP-111, 1973

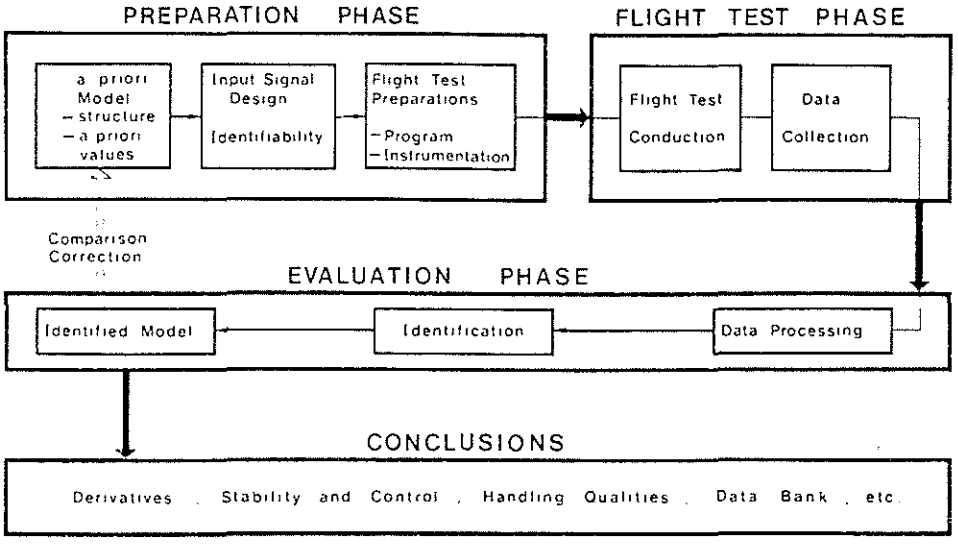

Figure 1: System identification procedure

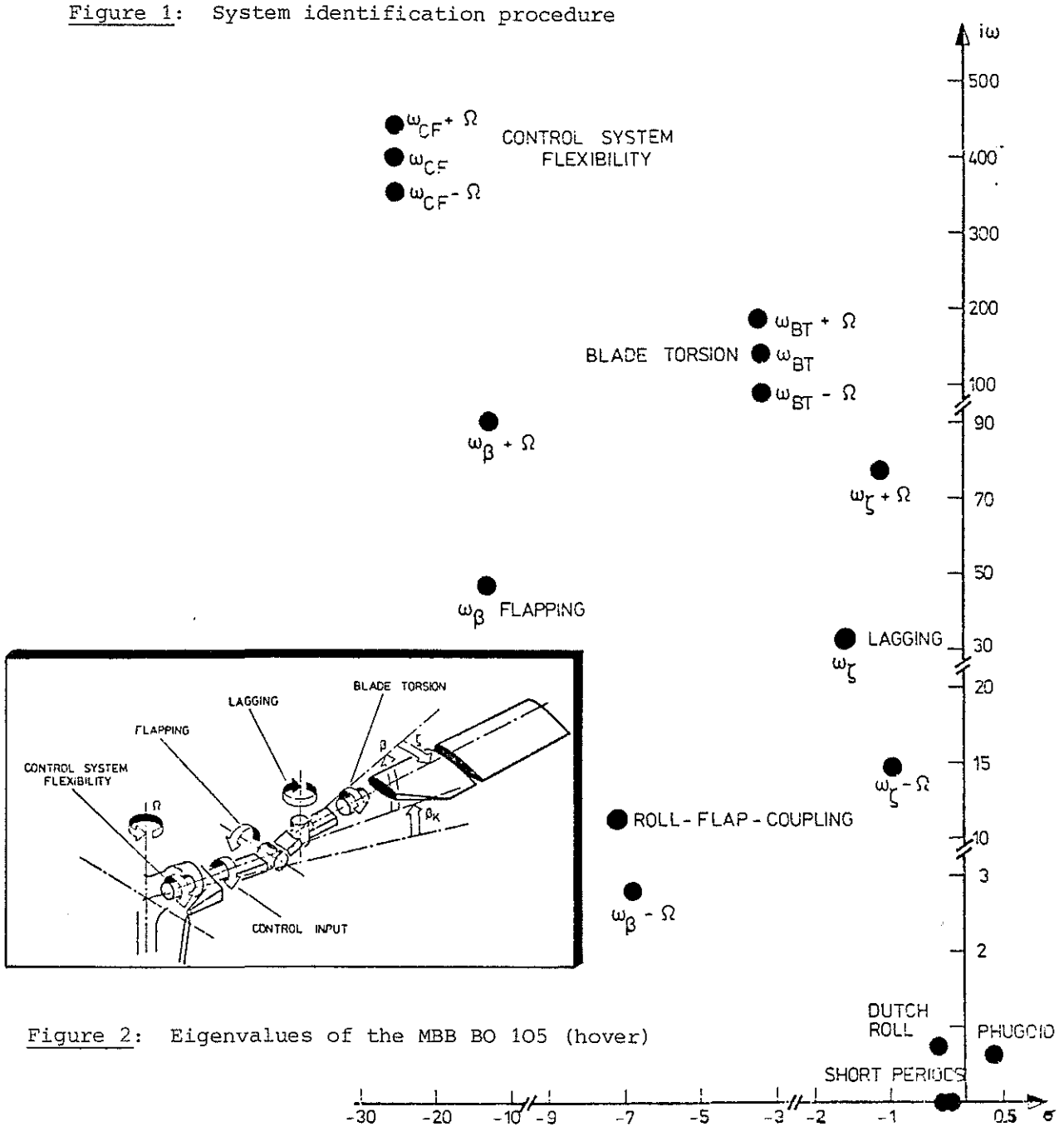

Figure 2: Eigenvalues of the MBB BO 105 (hover)

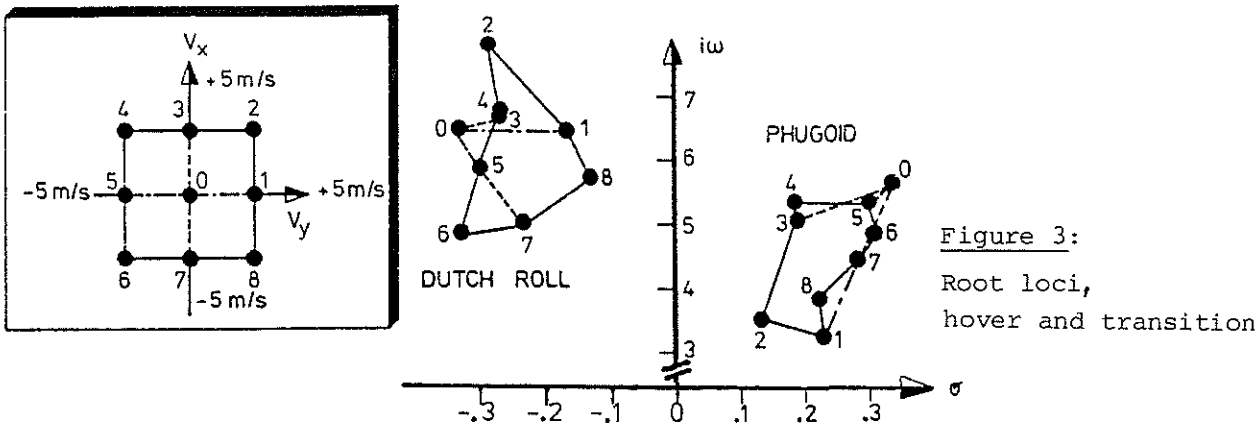

Figure 3:
Root loci,
hover and transition

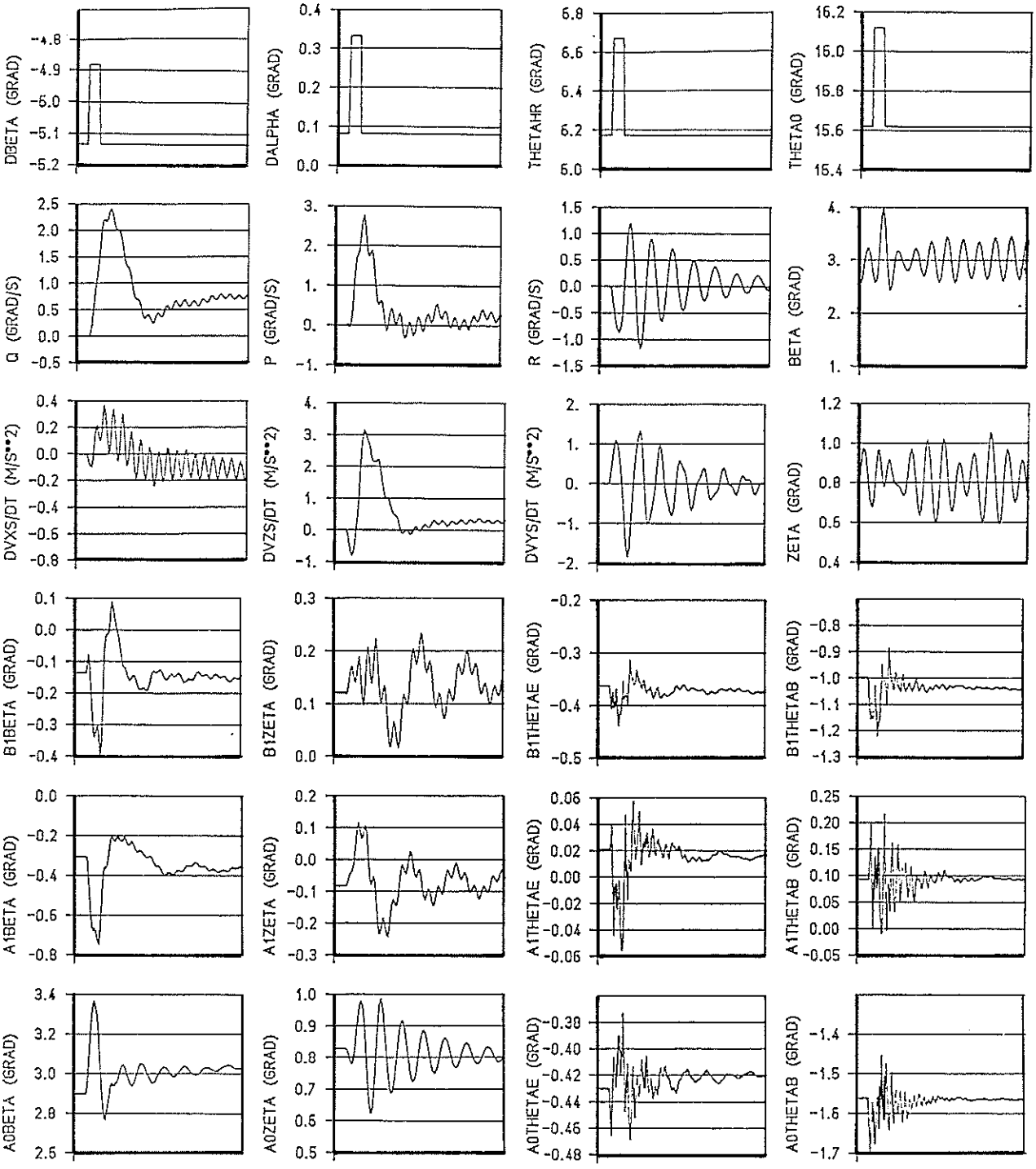

Figure 4: Time histories of rotorcraft with rotor dynamics included

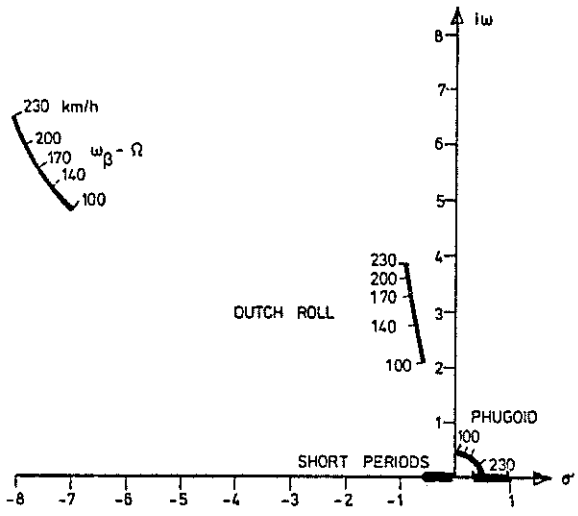

Figure 5:

Root loci of forward flight

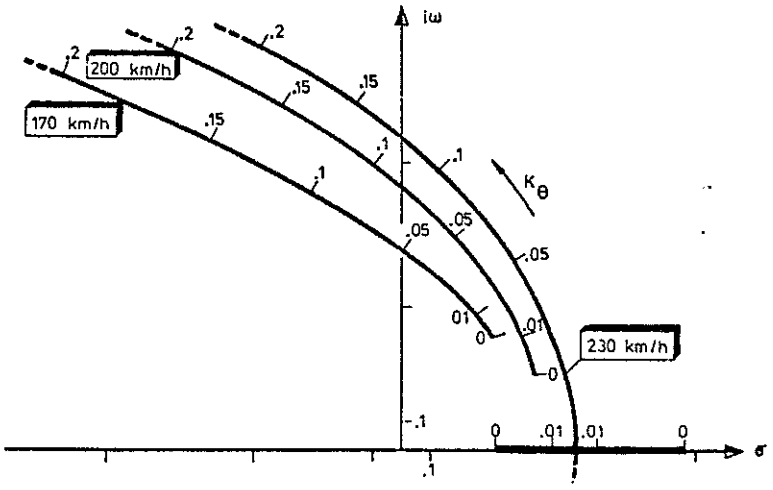

Figure 6:

Phugoid mode,
variation of amplification
factor and velocity

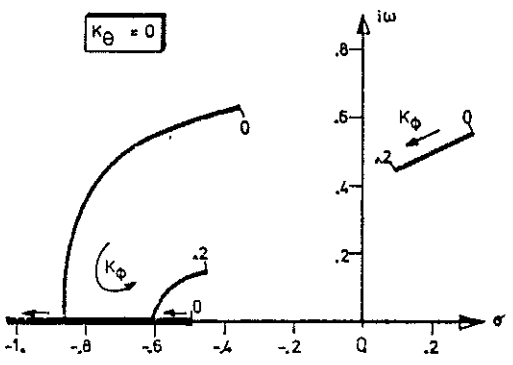

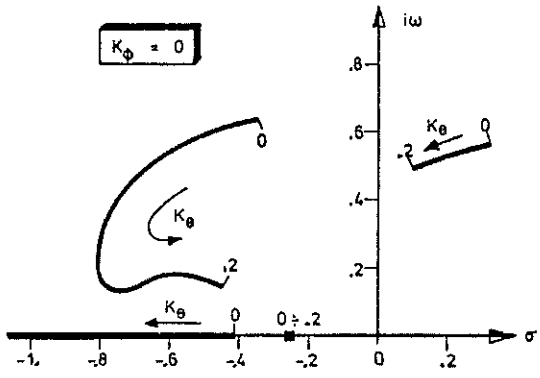

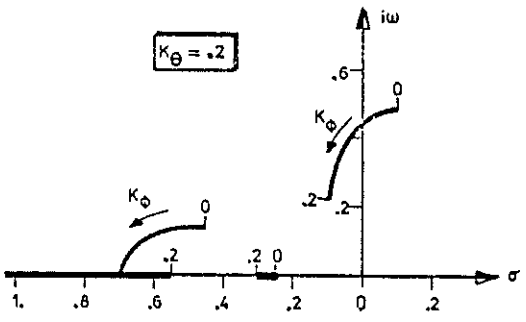

Figure 7:

Root locus diagrams,
varying amplification factors

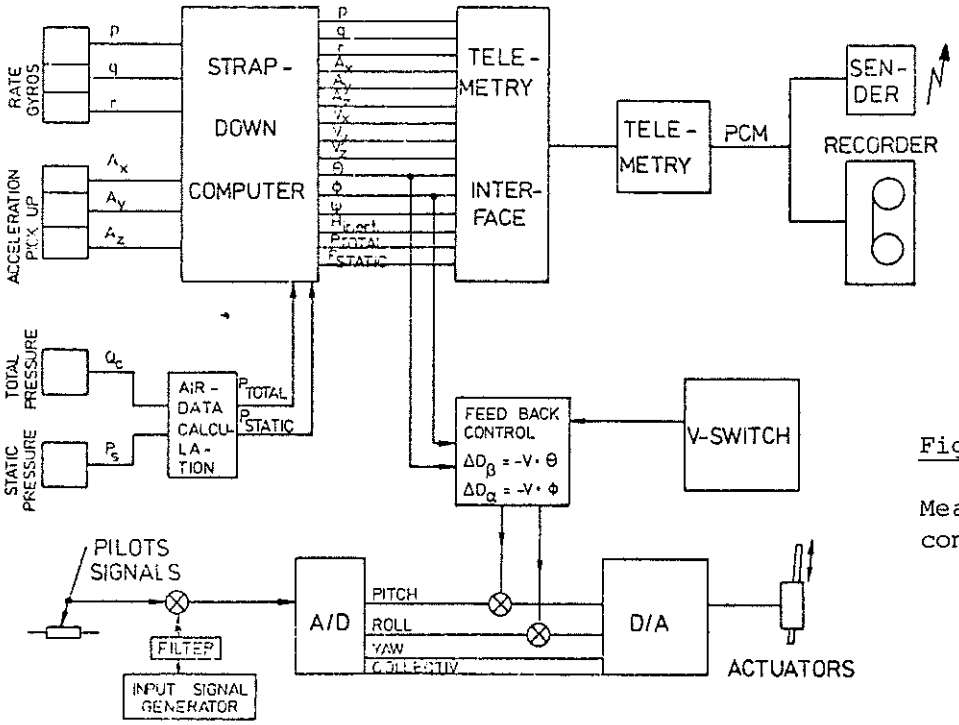

Figure 8:

Measuring and feedback control equipment

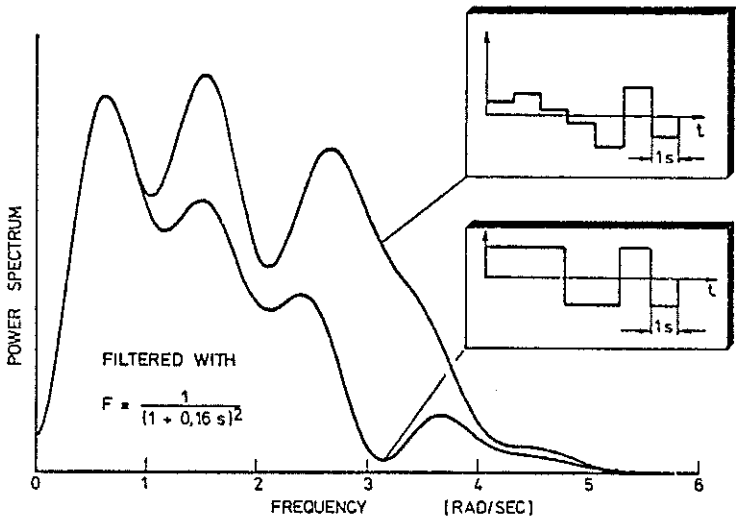

Figure 9:

Power spectra of optimized input signals

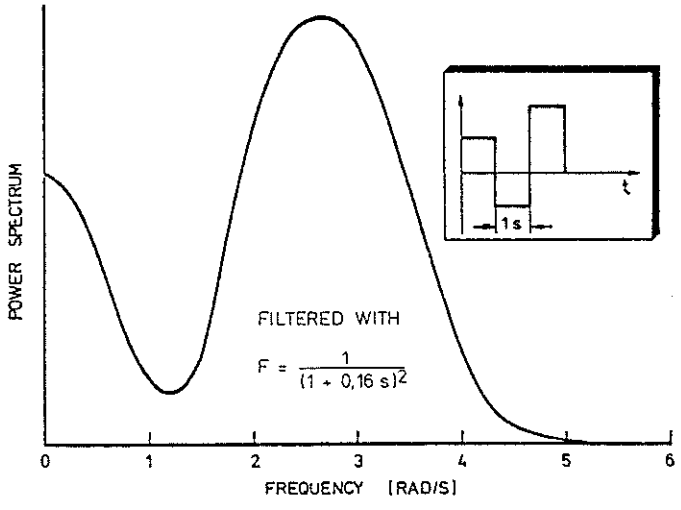

Figure 10:

Power spectrum of an input signal for feedback controlled systems

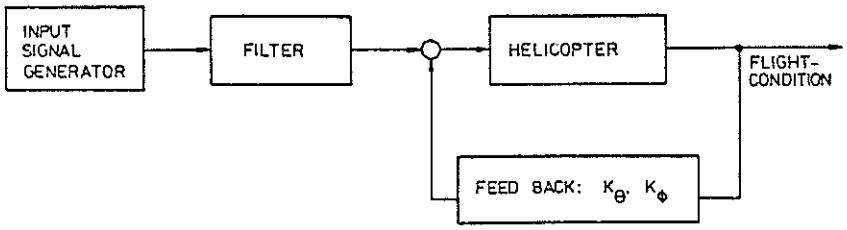

Figure 11: Feedback control and control input signal arrangement

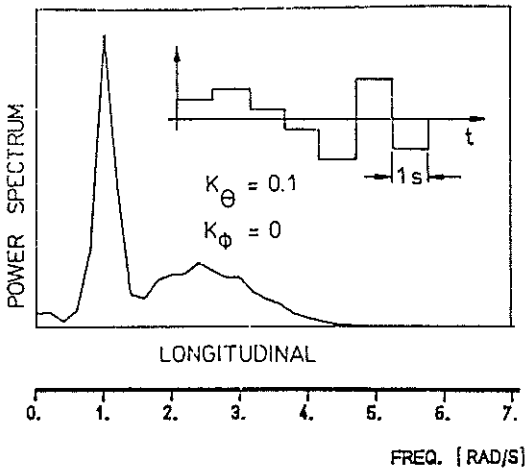

Figure 12

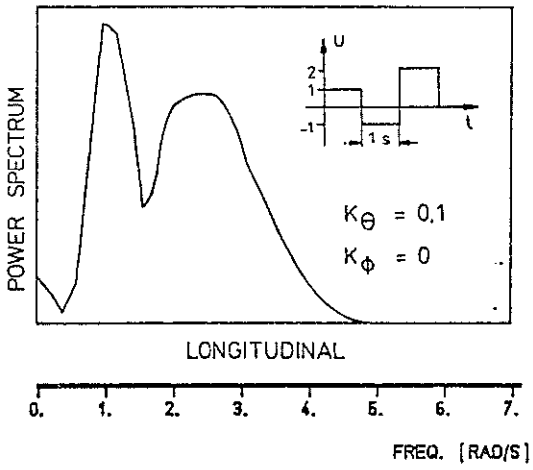

Figure 13

Power spectra of optimized input signals with feedback control (200 km/h)

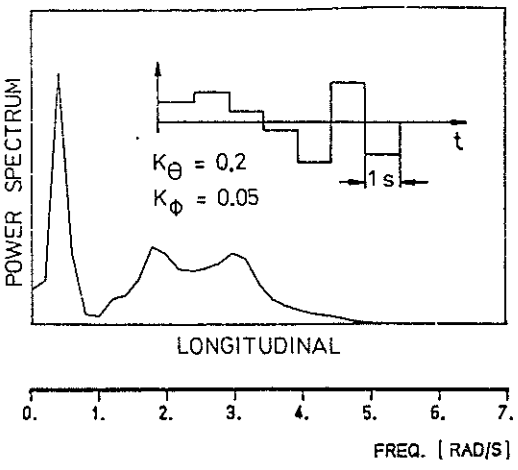

Figure 14

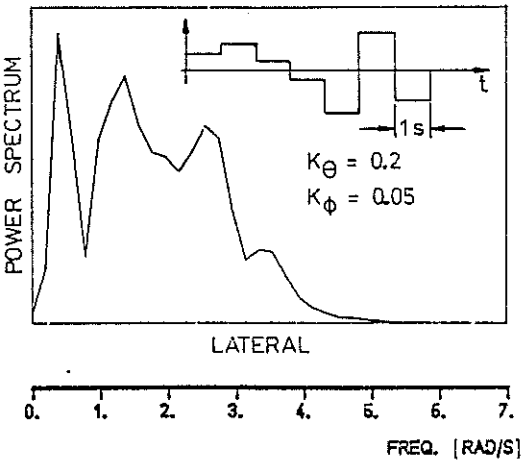

Figure 15

Power spectra of optimized input signals with feedback control (hover)

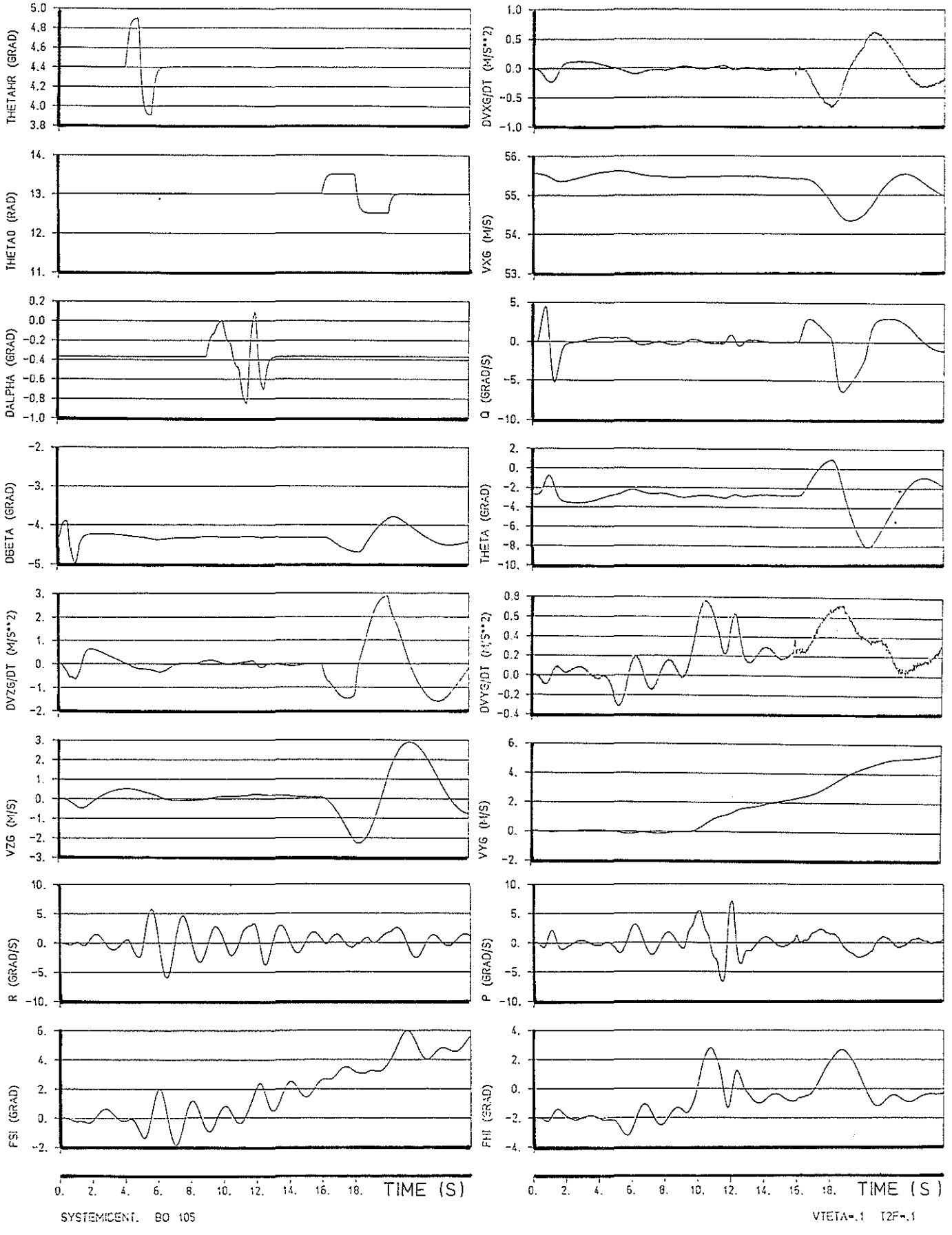

Figure 16: Time histories of simulation (200 km/h)

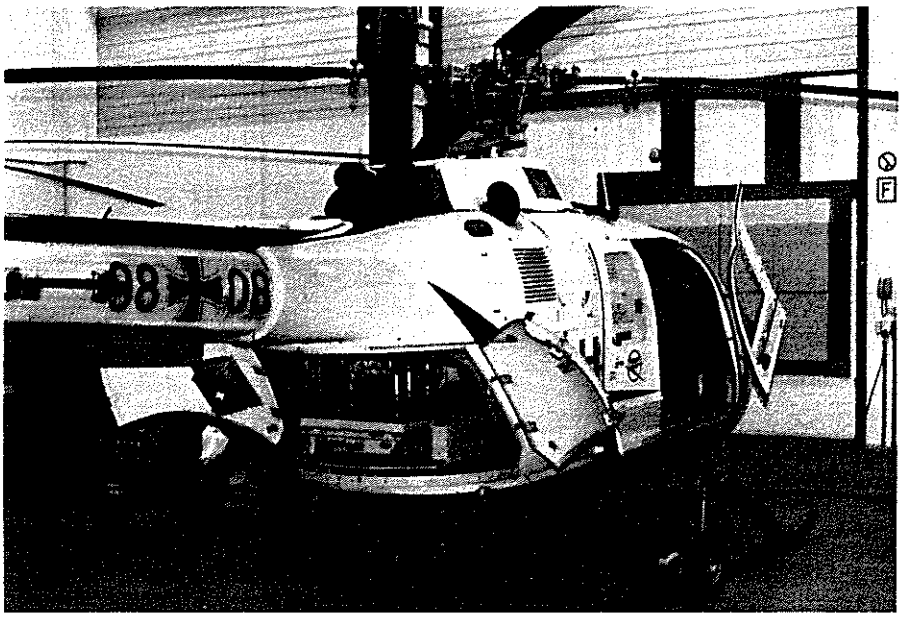

Figure 17: MBB BO 105 test vehicle with installed measuring equipment

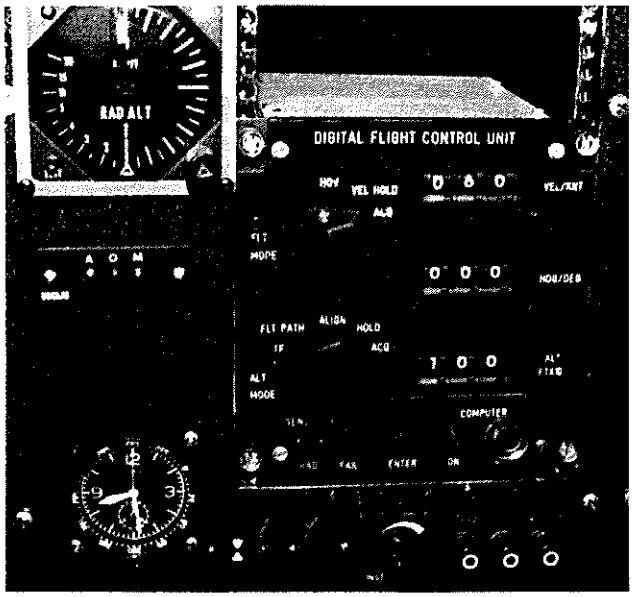

Figure 18:

Control unit for variable amplification factors

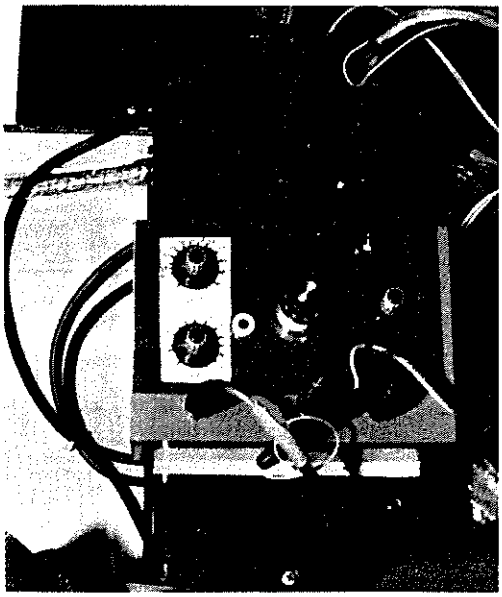

Figure 19:

Input signal generation and filtering unit

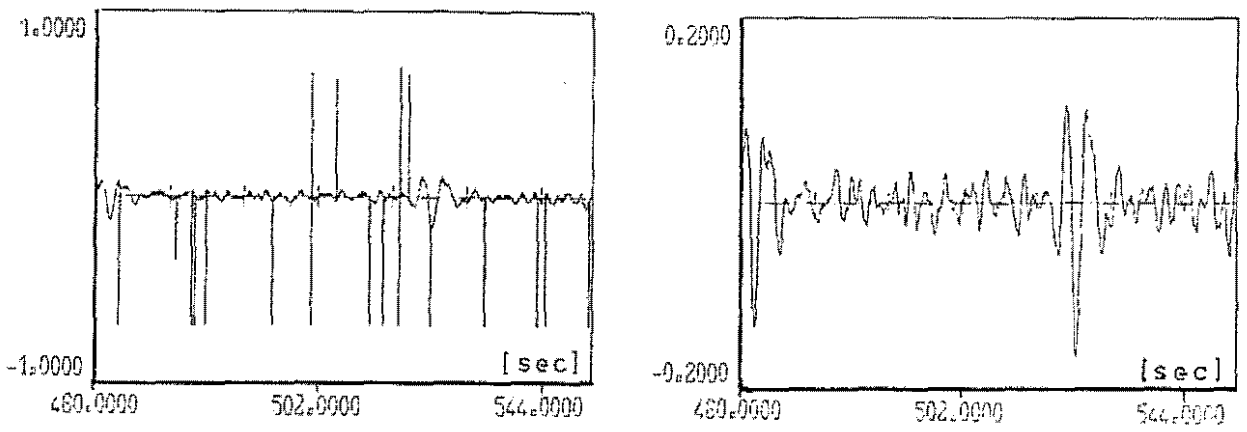

Figure 20: Drop outs and filtered flight test data of pitch rate (rad/s)

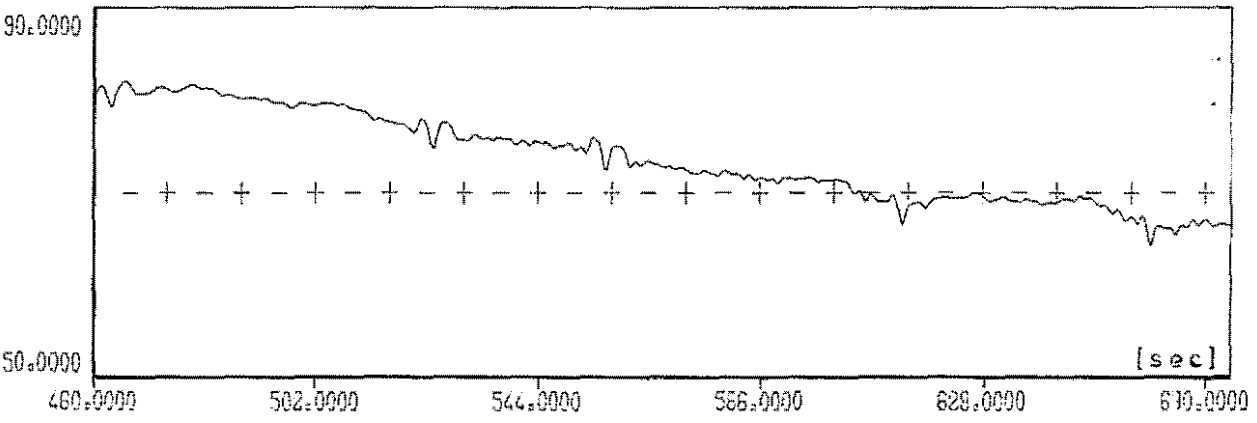

Figure 21: Typical drift of horizontal velocity u (m/s)

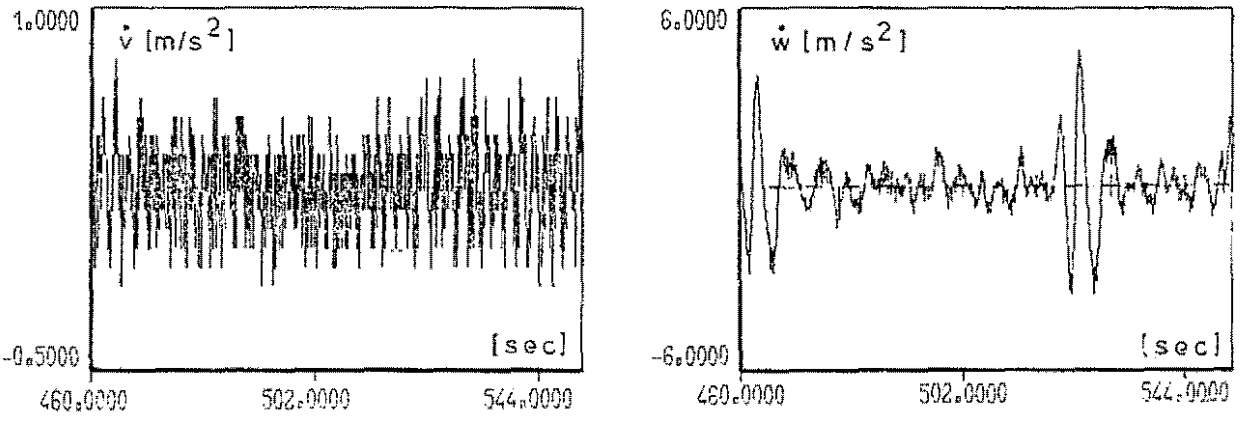

Figure 22: Typical acceleration data of flight test

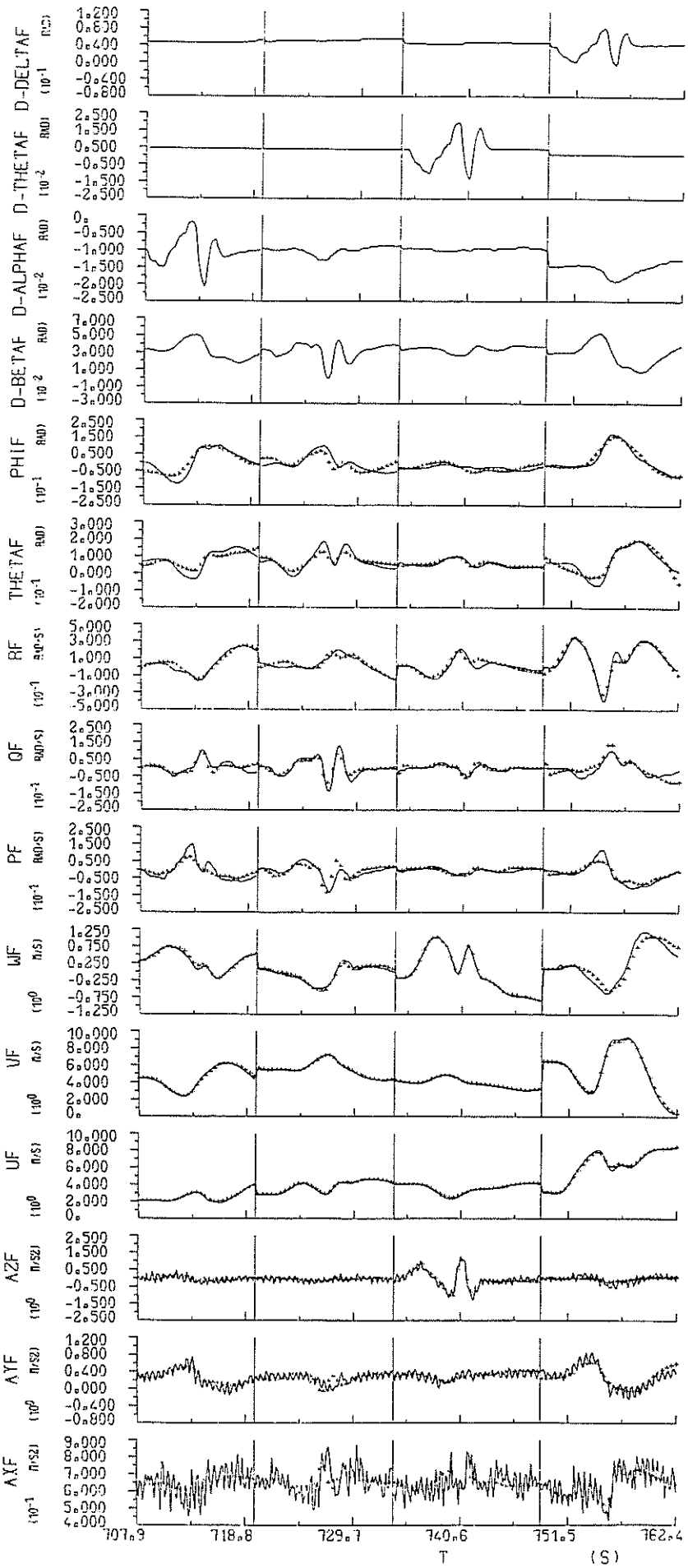

Figure 23: Time histories (hover) - flight test data +++ ML-identification

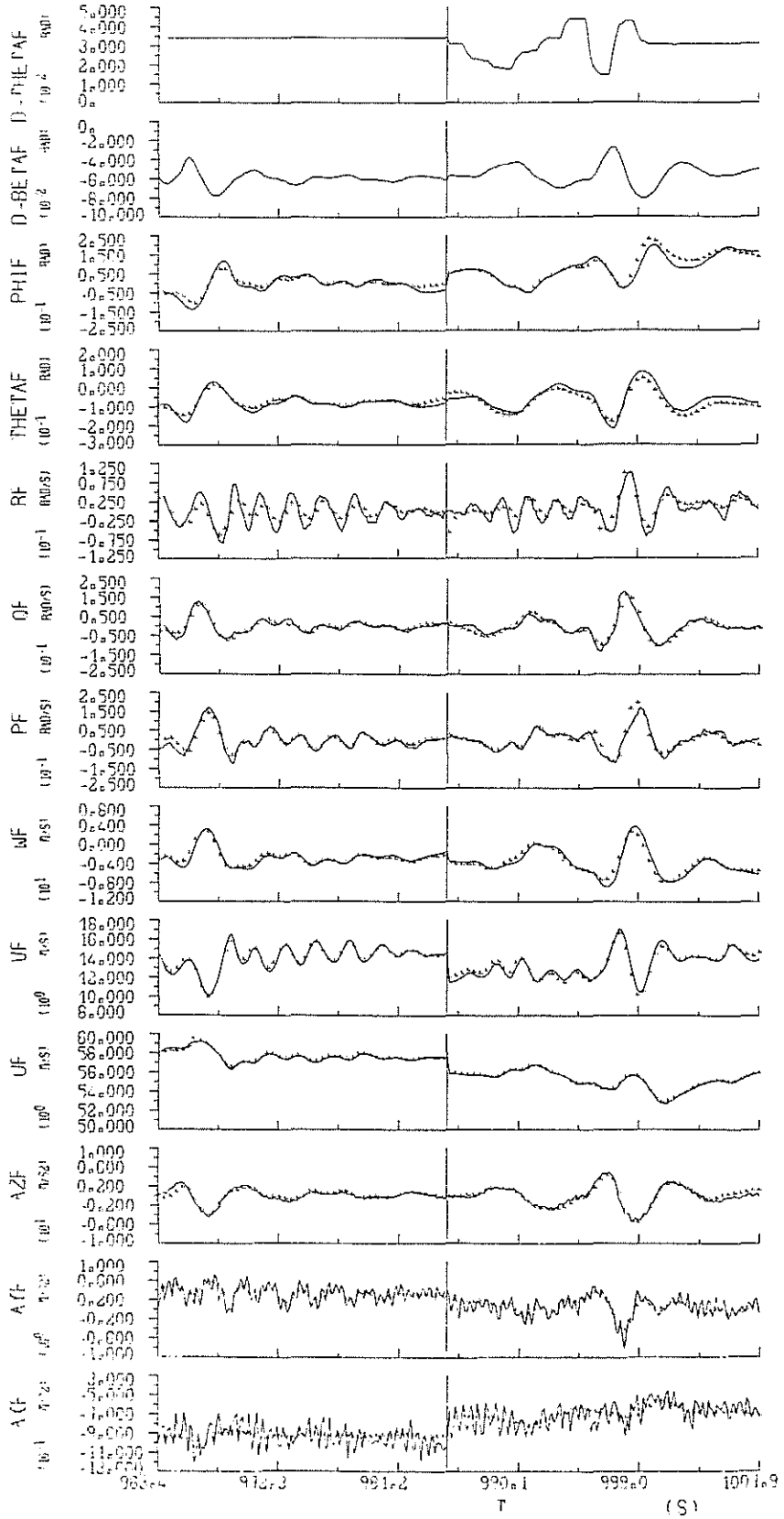

Figure 24: Time histories (200 km/h) - flight test data +++ ML-identification

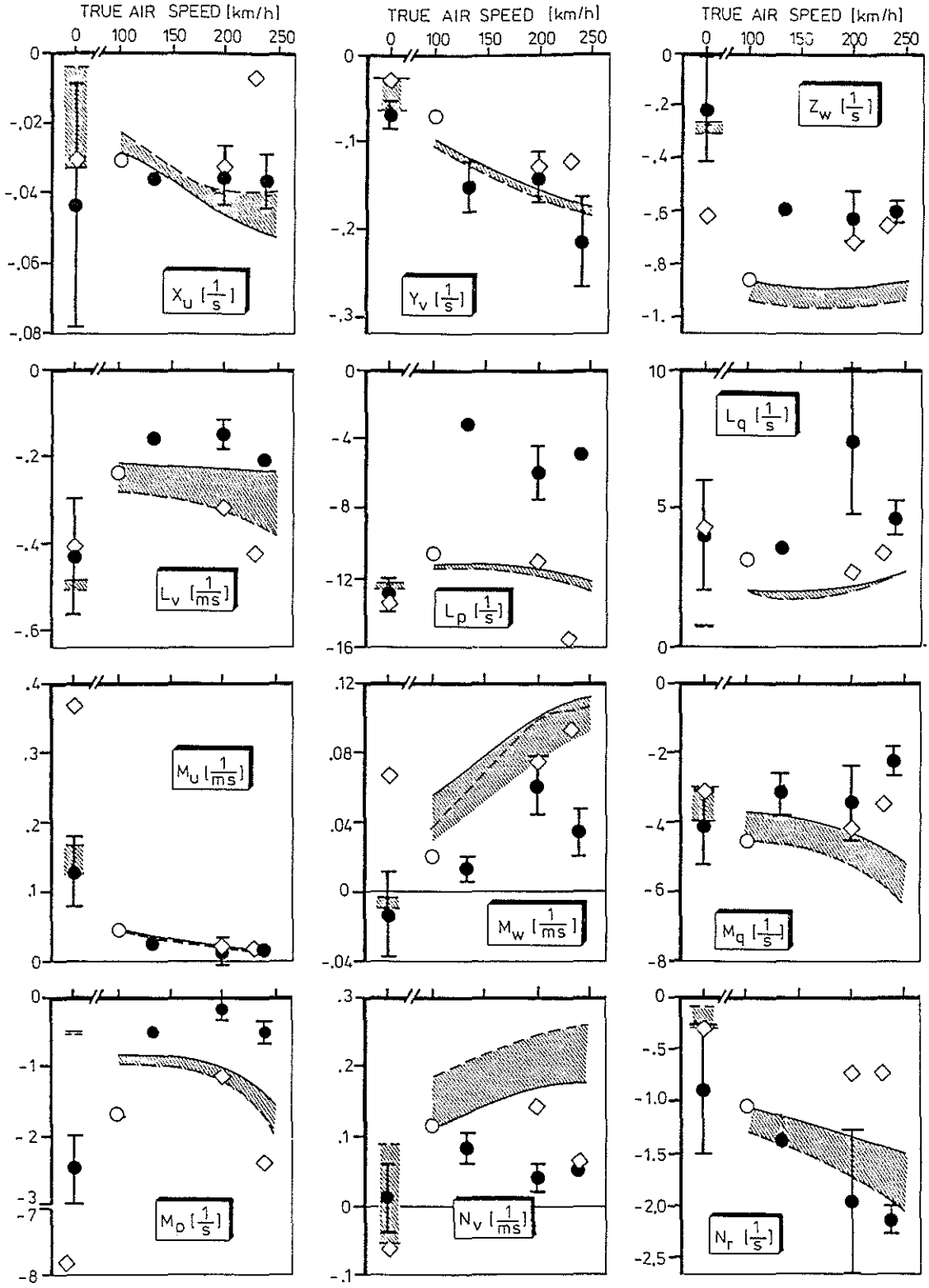

theoretical calculations
dashed line: gross weight 2100 kg, forward c.g. position
solid line: gross weight 2300 kg, mid c.g. position

◇ Identified from simulation, nonlinear model (2300 kg/mid c.g.)

○ Identified from simulation, nonlinear model (2100 kg/forward c.g.)

● Identified from flight test data (● small standard deviation)

Figure 25 Comparison of MBB-BO 105 identification results with theoretical calculations